Supplementary Information (SI) for Physical Chemistry Chemical Physics.
This journal is © the Owner Societies 2026

Supporting Information

Origin of Hydrogen Evolution Activity of Single-Atom Metals Anchored on Stone–Wales Defective Graphene: A First-Principles Study

Rui Sun, Zhongxu Wang*, Lei Chen*, Jingxiang Zhao

College of Chemistry and Chemical Engineering, and Key Laboratory of Photonic and Electronic Bandgap Materials, Ministry of Education, Harbin Normal University, Harbin 150025, China

* *To whom correspondence should be addressed. Email: wzx_azsecho@163.com (Z. Wang)*

Table S1. The computed binding energies (eV) of TMs adsorbed at three typical sites

on the SW-G monolayer, and the Bader charge transfer (e) at the most stable site (red value) are also presented.

TM	Five membered rings	Seven membered rings	Bridge site	Charge transfer
Ti	-5.31	-5.10	-5.26	-1.14
V	-2.64	-2.24	-2.59	-0.99
Cr	-1.50	-1.19	-0.39	-0.87
Mn	-0.09	0.26	-0.05	-0.68
Fe	-1.66	-1.61	-1.62	-0.61
Co	-2.23	-1.91	-2.18	-0.58
Ni	-2.47	-2.34	-2.23	-0.52
Cu	-1.19	-1.21	-1.21	-0.20
Zr	-3.53	-3.24	-4.01	-1.10
Nb	-3.24	-2.71	-3.47	-1.06
Mo	-1.97	-1.41	-1.85	-0.82
Ru	-2.83	-2.38	-2.75	-0.44
Rh	-2.99	-2.62	-2.77	-0.29
Pd	-1.27	-0.60	-1.47	-0.27
Ag	0.97	0.58	0.58	-0.20
Hf	-3.68	-3.14	-3.57	-1.07
Ta	-3.67	-3.12	-3.41	-0.89
W	-2.74	-1.90	-2.51	-0.74
Os	-2.34	-1.85	-1.96	-0.38
Ir	-2.43	-2.07	-1.47	-0.14
Pt	-2.86	-1.64	-2.95	-0.02
Au	0.25	-0.08	-1.21	0.12

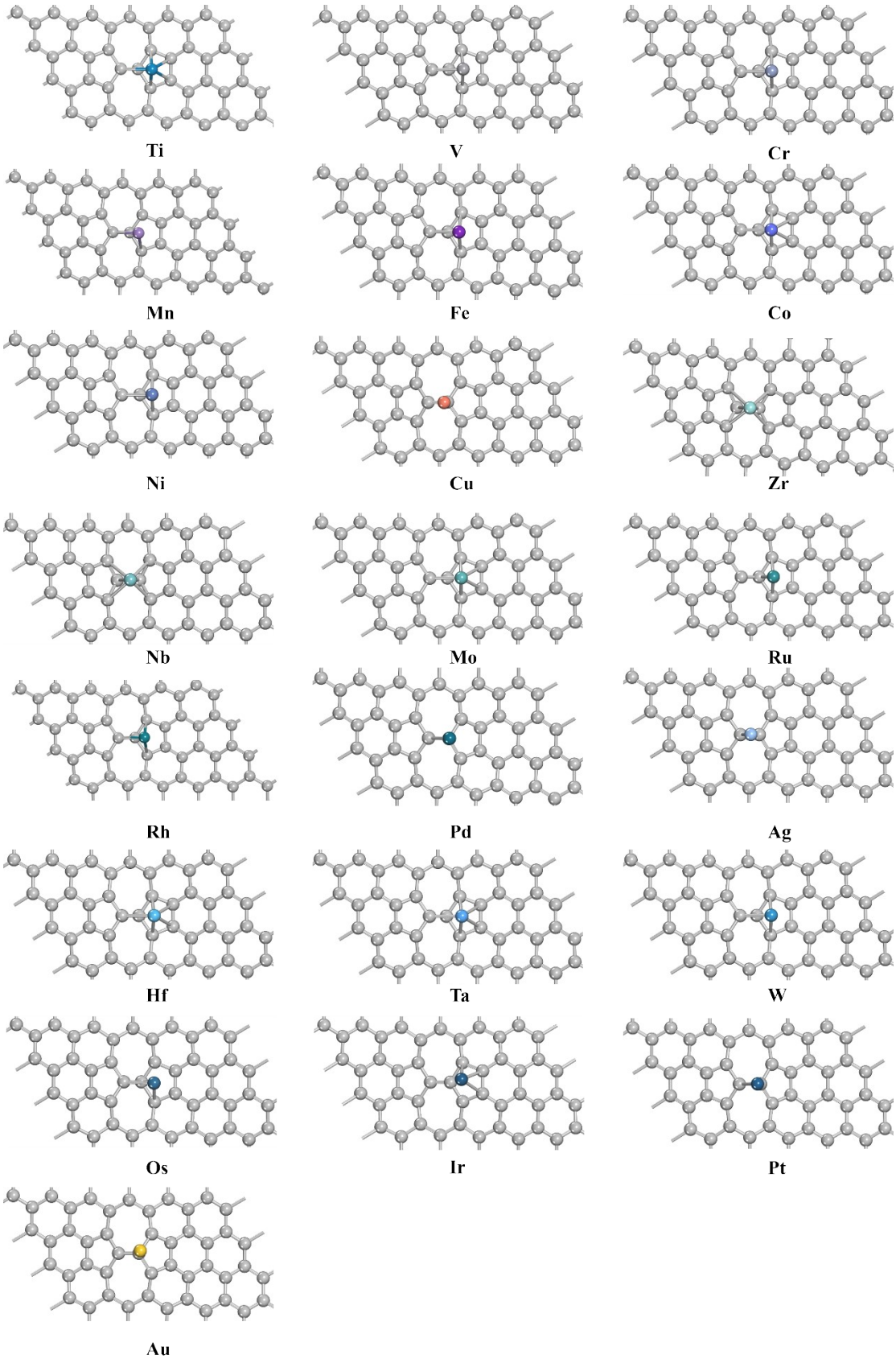

Fig. S1. Optimized geometrical structures of TM@SW-G systems.

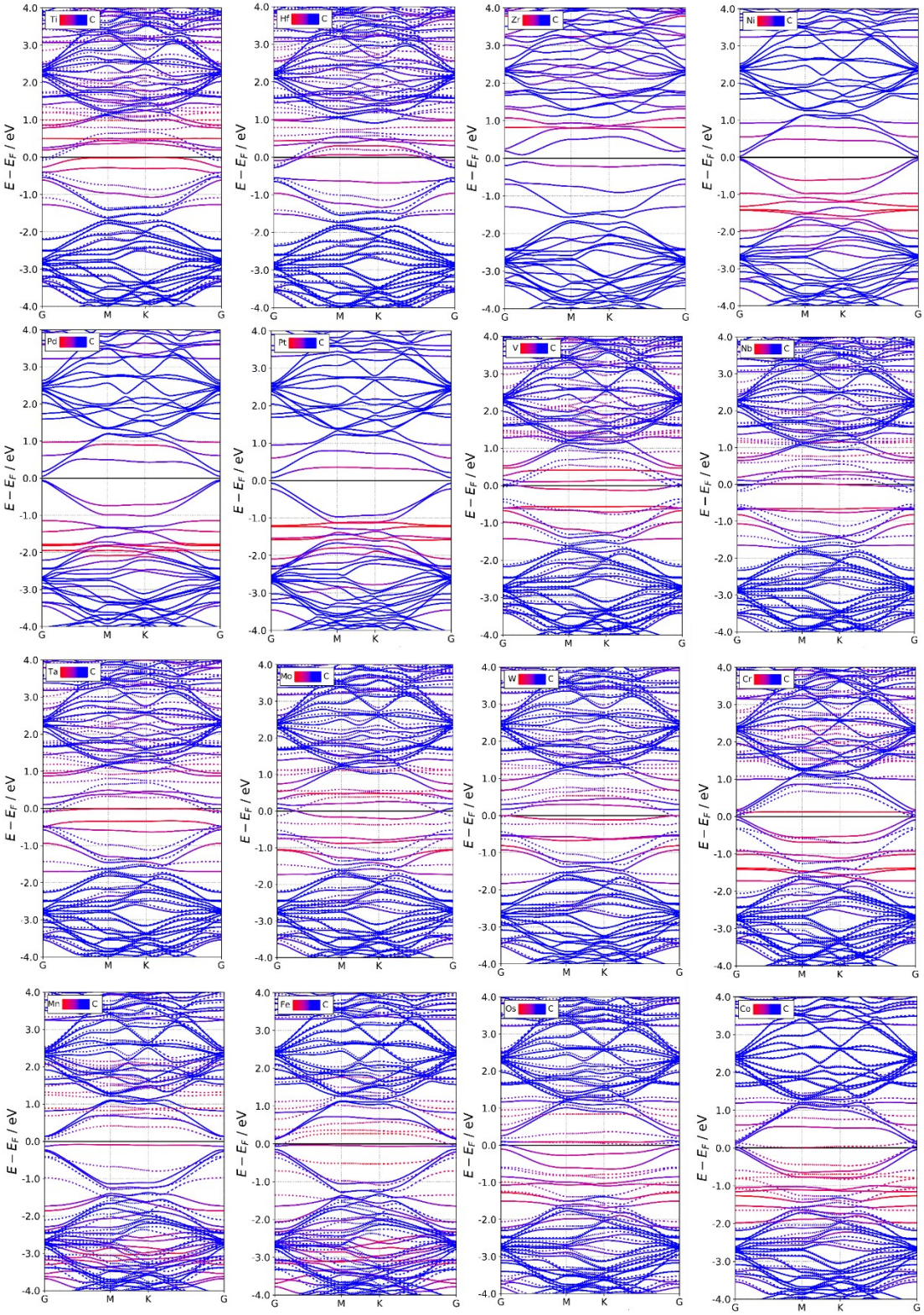
Ti C
Hf C
Zr C
Ni C
Pd C
Pt C
V C
Nb C
Ta C
Mo C
W C
Cr C
Mn C
Fe C
Os C
Co C
$E - E_F$ / eV
4.0
3.0
2.0
1.0
0.0
-1.0
-2.0
-3.0
-4.0
G
M
K
G

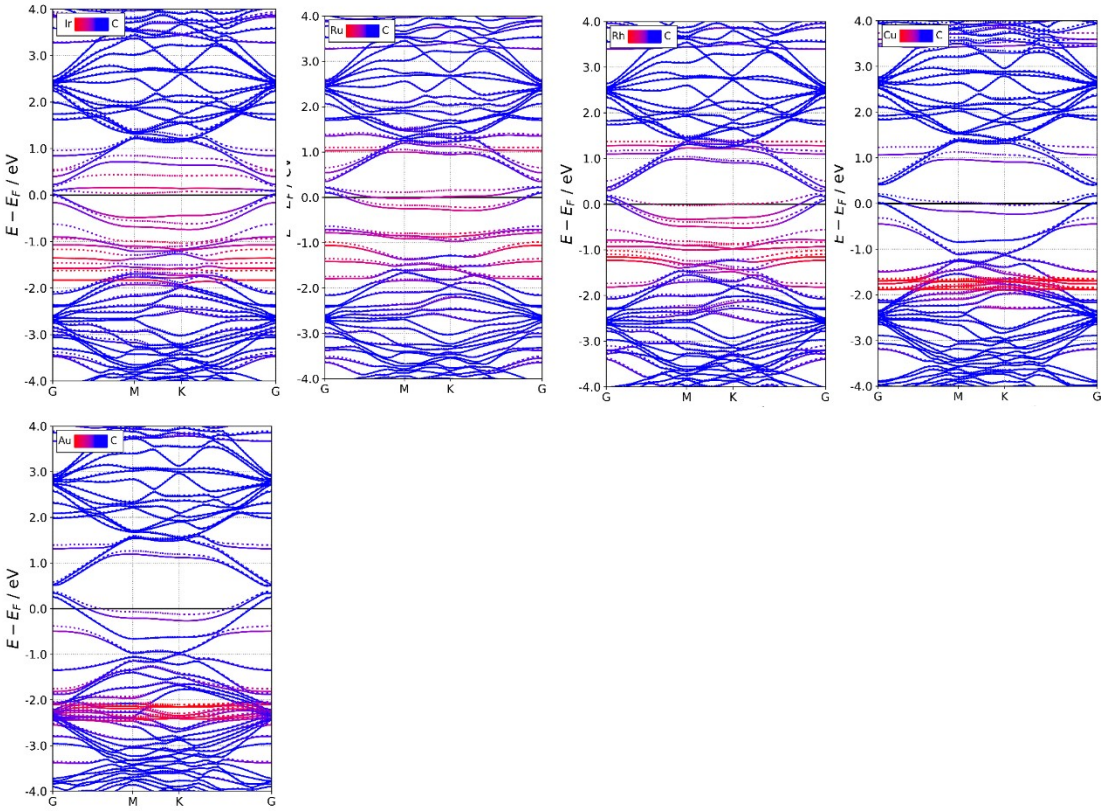

Fig. S2. The computed band structure of TM@SW-G systems.

Table S2. Calculated hydrogen adsorption Gibbs free energies (ΔG_{H^*}) of all investigated SACs with and without implicit solvent effect.

TM	with explicit solvent		without solvent	
	ΔE_{H^*}	ΔG_{H^*}	ΔE_{H^*}	ΔG_{H^*}
Ti	−0.51	−0.27	−0.50	−0.26
V	−0.33	−0.09	−0.23	0.01
Cr	0.48	0.72	0.60	0.84
Mn	−0.28	−0.04	−0.18	0.06
Fe	2.11	2.35	2.06	2.30
Co	0.33	0.57	0.50	0.74
Ni	−0.35	−0.11	−0.43	−0.19
Cu	0.61	0.85	0.56	0.80
Zr	−0.37	−0.13	−0.39	−0.15
Nb	−0.91	−0.67	−0.83	−0.59
Mo	−0.74	−0.50	−0.80	−0.56
Ru	−0.71	−0.47	−0.69	−0.45
Rh	−0.39	−0.15	−0.43	−0.19
Pd	0.51	0.75	0.48	0.72
Hf	−0.77	−0.53	−0.90	−0.66
Ta	−1.24	−1.00	−1.08	−0.84
W	−0.67	−0.43	−0.74	−0.50
Os	−1.41	−1.17	−1.36	−1.12
Ir	0.41	0.65	0.40	0.64
Pt	1.66	1.90	1.43	1.67
Au	0.61	0.85	0.50	0.74

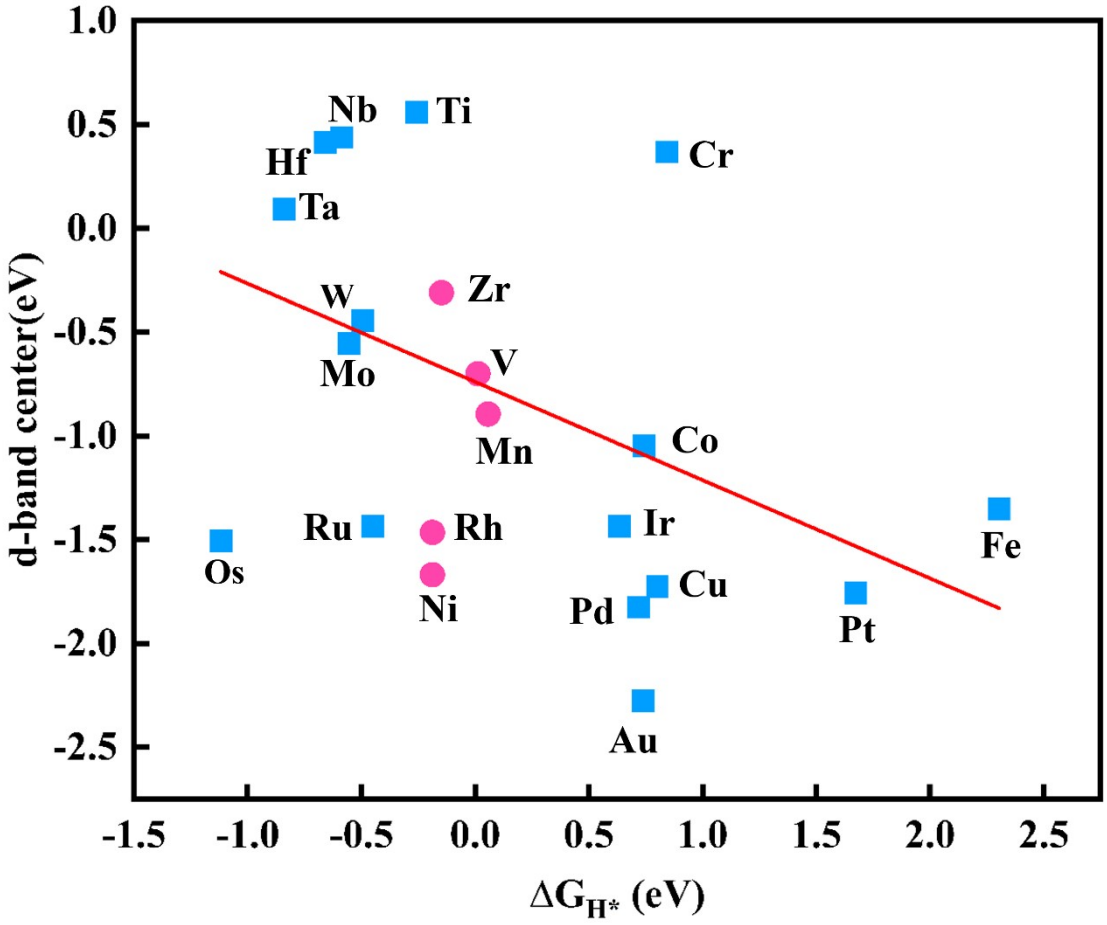

Fig. S3. The correlation between the ΔG_{H*} of hydrogen adsorption and the d-band center.

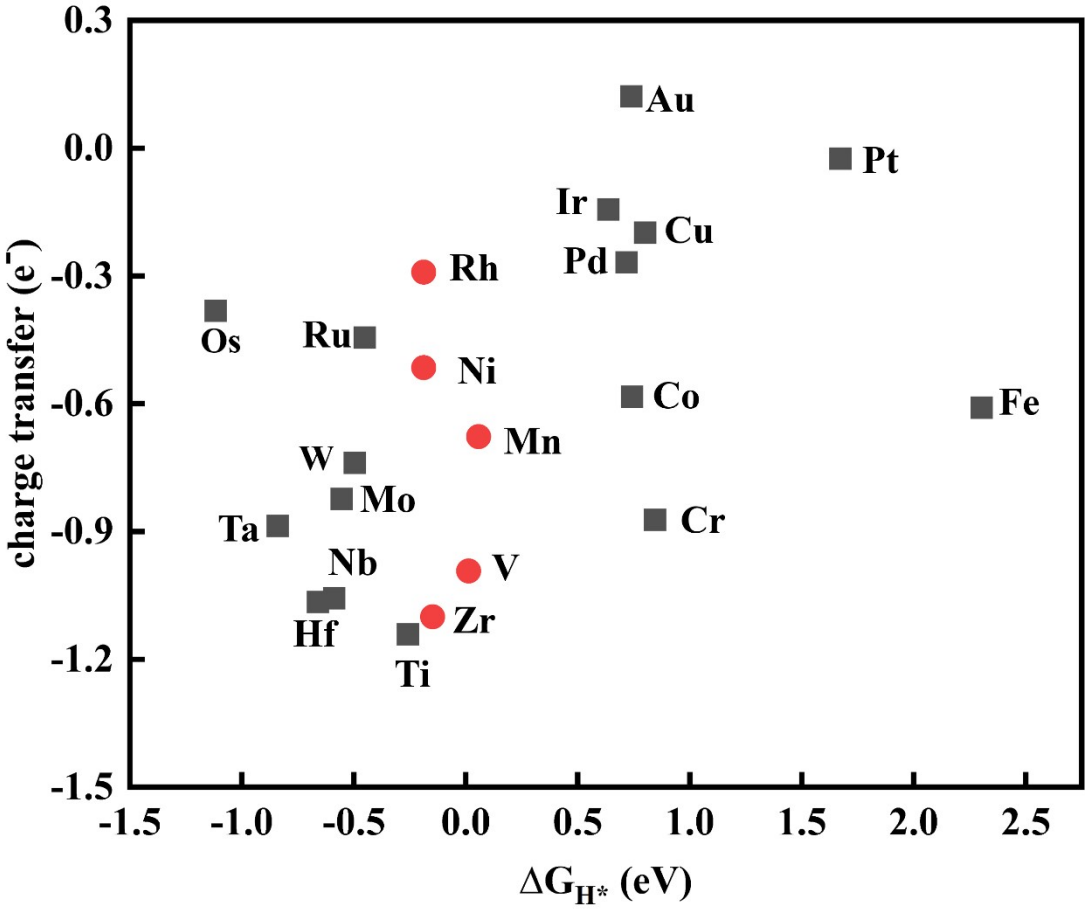

Fig. S4. The correlation between the ΔG_{H*} of hydrogen adsorption and the Bader charge.

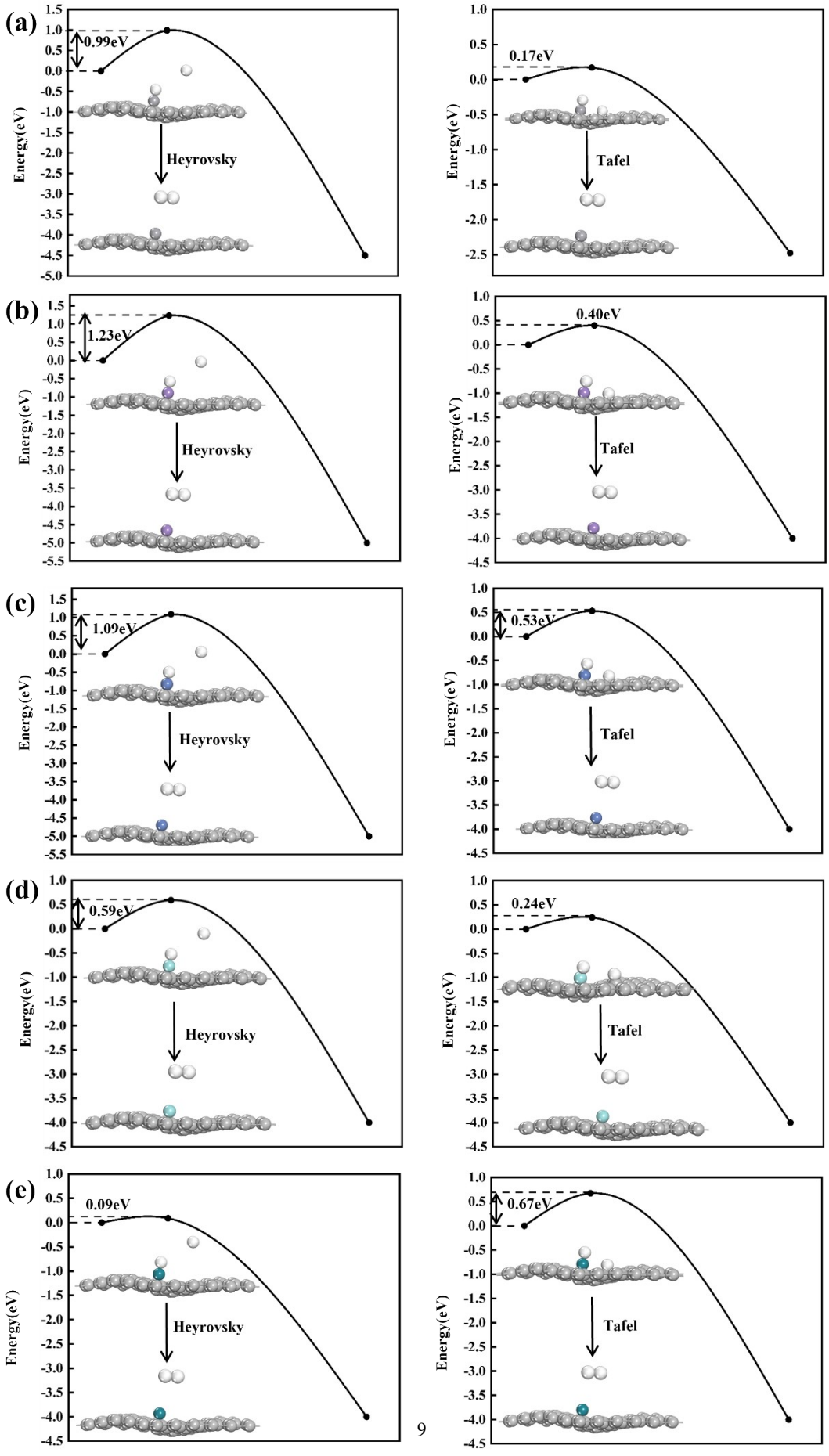
(a)
0.99eV
Heyrovsky
0.17eV
Tafel
(b)
1.23eV
Heyrovsky
0.40eV
Tafel
(c)
1.09eV
Heyrovsky
0.53eV
Tafel
(d)
0.59eV
Heyrovsky
0.24eV
Tafel
(e)
0.09eV
Heyrovsky
0.67eV
Tafel
Energy(eV)

Fig. S5. The minimum-energy pathways and the corresponding barriers of the Heyrovsky and Tafel reactions on (a) V@SW-G, (b) Mn@SW-G, (c) Ni@SW-G, Zr@SW-G, and (d) Rh@SW-G.

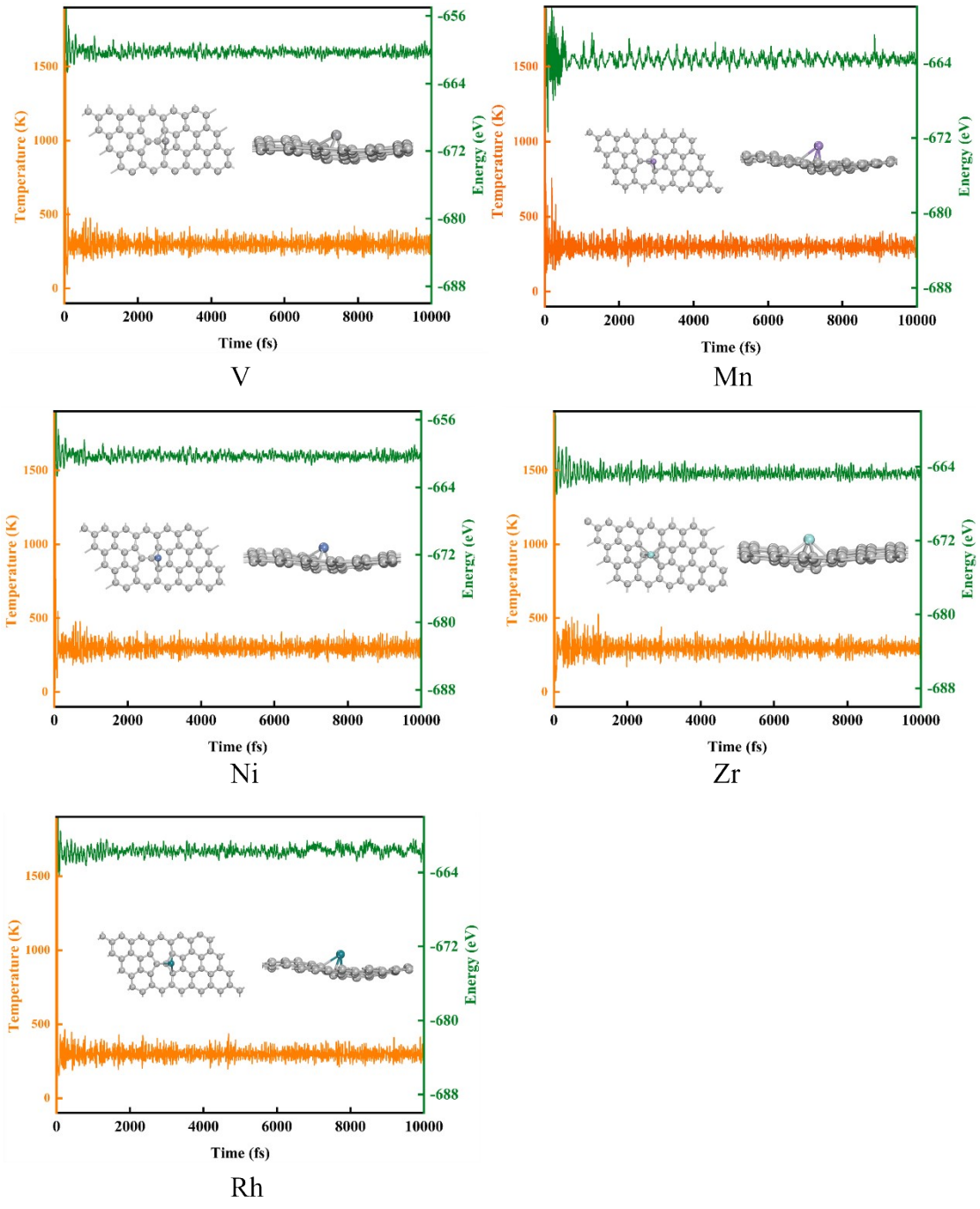

Fig. S6. Energy and temperature evolution versus the AIMD time for TM@SW-G.